The Astrophysical Journal, 579:716–724, 2002 November 10

QUIESCENT HIGH-ENERGY GAMMA-RAY EMISSION FROM SOFT GAMMA-RAY REPEATERS

L. Zhang[1,2] and K. S. Cheng[1]

Received 2001 December 6; accepted 2002 July 12

ABSTRACT

We present a model for the high-energy γ-ray emission from the outer gap of soft gamma-ray repeaters (SGRs) during their quiescent states. In this model, X-rays come from the stellar surface, but the emerging X-ray spectrum will have a power-law tail because of the multiple scattering at the cyclotron resonance in the magnetosphere, as pointed out by Thompson, Lyukitov, & Kulkarni. The outer gap is sustained by the collision between these X-rays with the high-energy photons produced in the outer gap through the photon-photon pair production. We have taken a magnetic dipole geometry into account in estimating the fractional size of the outer gap. The fractional size of the outer gap depends on the period, surface magnetic field, average X-ray energy, and the magnetic inclination angle of the neutron star. After the average fractional size outer gap is determined, the spectrum and luminosity of high-energy photons from the outer gap can be calculated. We apply this model to some SGRs, such as SGR 1806−20 and SGR 1900+14, and compare the expected integral fluxes with the sensitivities of EGRET, GLAST, MAGIC, and VERITAS. We predict that the integral flux of SGR 1900+14 may be greater than the sensitivity of GLAST, and especially that the integral flux for a large magnetic inclination angle (say 80°) may be greater than the sensitivities of GLAST and MAGIC. However, we predict that SGR 1806−20 would not be detected by GLAST because its distance is about 3 times of that of SGR 1900+14.

Subject headings: gamma rays: theory — pulsars: general — stars: neutron

1. INTRODUCTION

The soft gamma-ray repeaters (SGRs) are a small group of radio-quiet soft X-ray pulsars characterized by long rotation periods of 5–8 s and large spin-down rates (e.g., Mereghetti & Stella 1995; Kouveliotou et al. 1998, 1999). Four SGRs (1806−20, 1900+14, 0525−66, and 1627−41) have now been identified, and a fifth (SGR 1801−23) has possibly been detected (for an observational review, see Hurley et al. 2000). Observationally, SGRs have two states, burst and quiescence. During the burst state, SGRs have intense and repeated emission of soft ($kT \leq 30$ keV) γ-rays. These bursts are significantly super-Eddington ($\geq 10^3 L_{\rm Edd}$). Four identified SGRs have been detected to emit persistent X-rays. The pulsations during the quiescent state have been detected from three SGRs. All SGRs are associated with supernova remnants, indicating that they are young objects. In their quiescent emission, SGRs share many common properties with anomalous X-ray pulsars (AXPs): similar X-ray luminosities ($L_{\rm X} \sim 3 \times 10^{34}$–$10^{36}$ ergs s^{-1}) and spin periods ($P \sim 6$–12 s). However, there are also some differences between SGRs during their quiescent state and AXPs. SGRs spin down even more rapidly than AXPs. Furthermore, AXPs appear to have softer X-ray spectra than the persistent SGR emission. The quiescent X-ray spectra of SGRs display a power-law spectrum with photon index of $\sim$2 and may also have small blackbody contributions with $kT \sim 0.5$ keV, while AXP X-ray spectra are characterized by the sum of a steep power law with a photon index of $\sim$3–4 and an blackbody-like components with a temperature of $\sim$0.4–0.6 keV (e.g., Perna et al. 2001; Marsden & White 2001).

Theoretically, the magnetar model (Duncan & Thompson 1992) has been proposed to explain the AXPs and SGRs. In the magnetar model, the long periods P and high spin-down rates $\dot{P}$ are due to the magnetic braking of a surface dipolar magnetic field of the order 10^{14} to $\sim 10^{16}$ G, and the pulsed X-ray emission could be powered by magnetic field decay (Thompson & Duncan 1996; Kouveliotou et al. 1998; Heyl & Kulkarni 1998). Recently, Thompson, Lyutikov, & Kulkarni (2002) have considered the electrodynamics of magnetars. They pointed out that the thermal X-ray spectrum from the stellar surface will be redistributed as a result of multiple scattering at the cyclotron resonance in the magnetar magnetosphere, so that the emerging X-ray spectrum will have a nonthermal tail. The difference between the spectra of the SGRs and AXPs is due to the fact that the softest AXP spectra correspond to external magnetic fields, which carry relative weak electrical currents, and the hardest SGR spectra correspond to magnetospheres, which are strongly twisted. In the magnetar magnetosphere in which the magnetic field strength exceeds the quantum critical field strength, $B_c = m_e^2 c^3 / e\hbar \approx 4.4 \times 10^{13}$ G, γ-ray photons will be split into two lower energy photons before they are materialized to electron-positron pairs in reaction with the strong magnetic fields (e.g., Baring & Harding 2001; Zhang 2001); then the γ-ray emission rooted at the polar caps will be quenched. However, in the outer gap, which is far away from the pulsar surface, the γ-rays will be emitted because the local magnetic field will drop below the quantum critical value. Cheng & Zhang (2001) have studied high-energy γ-ray emission from the outer magnetospheres of the AXPs. In their model, the soft photons that sustain the outer gap are the thermal X-ray photons from the stellar surface. They have approximated the typical energy ($kT_{\rm eff}$) of thermal X-rays as the X-ray typical energy. This approximation is reasonable for the AXPs because of the observed feature of X-ray spectra of the AXPs. As mentioned above,

[1] Department of Physics, University of Hong Kong, Hong Kong, China; lzhang@bohr.physics.hku.hk, hrspksc@khucc.hku.hk.
[2] Department of Physics, Yunnan University, Kunming, China.

however, X-ray spectral distributions of the SGRs are different from those of the AXPs. In such a case, the fractional size of the outer gap should be changed, and then the γ-ray emission should be changed for the SGRs during their quiescent state.

In this paper, we study the γ-ray emission from the outer magnetosphere of the SGRs during their quiescent states. The main differences between this model and the AXP model (Cheng & Zhang 2001) are as follows. First, we assume that the emerging X-ray spectrum consists of thermal and nonthermal X-rays, based on the observed data (e.g., Marsden & White 2001; Perna et al. 2001) and the model of Thompson et al. (2002) (see § 2.1), while X-rays for AXPs were assumed to be thermal in Cheng & Zhang (2001). We find that the luminosity ratio of thermal and nonthermal components and the spectral break and spectral index of the nonthermal component play vital roles in determining the γ-ray emission from SGRs. Second, we take the effect of magnetic inclination angle into account in estimating the fractional size of the outer gap; it turns out that this is also an important factor of the γ-ray spectrum (§ 2.2). In § 2.3, we derive the luminosity and spectrum of high-energy photons. We apply this model to individual SGRs in § 3, and a discussion is presented in § 4.

2. THE GAMMA-RAY EMISSION MODEL

2.1. *X-Ray Field*

Observationally, persistent X-ray spectra of SGR 1900+14 and SGR 1806−20 can be fitted by a two-component blackbody plus power spectral model (e.g., Marsden & White 2001; Perna et al. 2001). Using *ASCA* data, Marsden & White (2001) estimated the temperatures of the blackbody, the spectral indices of power law, and the ratio of the 2–10 keV power-law and bolometric blackbody luminosities. In the magnetar model, multiple scattering at the cyclotron resonance in the magnetar magnetosphere will redistribute photons in frequency, resulting in a nonthermal tail of the emerging X-rays (Thompson et al. 2002). Thompson et al. (2002) considered the structure of a neutron star magnetosphere threaded by large-scale electrical currents, which are supplied by ions and electrons. They have shown that: (1) the stellar surface is heated at a rate comparable to the observed luminosities of AXPs and SGRs. (2) Since ions with a mildly relativistic velocity and electrons with Lorentz factors of $\sim 10^3$–10^4 resonantly scatter 1–10 keV photons, multiple scattering at the cyclotron resonance by these charged carriers will result in a nonthermal spectral tail to the X-ray flux emerging from the surface, and the hardness of the nonthermal spectrum increases with the number of scattering, and thus with the resonant optical depth. (3) The upper cutoff to the nonthermal spectral tail depends on the species of charged particles. The nonthermal tail extends up to a energy $E_{\rm X,max} \geq 100$ keV in the case of electron cyclotron scattering and $E_{\rm X,max} \sim 30$ keV in the case of ion cyclotron scattering. (4) For either ion or electron cyclotron resonance, the optical depth $\tau(\theta)$ is anisotropic, vanishing toward the magnetic poles; the resonant surface is nonspherical; and the scattered radiation is beamed along the magnetic field. However, there is not a detailed calculation of the persistent X-ray spectra of the SGRs, so we construct an X-ray spectrum for a given SGR by using the fitting result and the idea proposed by Thompson et al. (2002) in their magnetar model. We assume that the emerging X-ray spectrum satisfies

$$F_{\rm X}(E_{\rm X}) = C\left\{ \frac{E_{\rm X}^2}{\exp(E_{\rm X}/E_0)-1} + \eta E^{-\alpha_{\rm X}}[\Theta(E_{\rm X}-E_1)-\Theta(E_{\rm X}-E_{\rm X,max})] \right\}, \quad (1)$$

where C is the normalized constant, which is estimated by using $L_{\rm X} = \int F_{\rm X}(E_{\rm X}) dE_{\rm X}$, $L_{\rm X}$ is the observed X-ray luminosity after correction of the interstellar absorption, $E_{\rm X}$ is the X-ray energy, $E_0 = kT$ and $\alpha_{\rm X}$ are the typical energy of the blackbody radiation and the spectral index of the power law, which can be estimated by fitting the observed data, η is a parameter that is determined by the observed ratio of the 2–10 keV power-law and bolometric blackbody luminosity $(L_{\rm PL}/L_{\rm BB})_{\rm obs}$, and $\Theta(x)$ is the step function. The parameter η depends on $L_{\rm PL}/L_{\rm BB}$, E_0, and $\alpha_{\rm X}$, but is not so sensitive to E_1 and $E_{\rm X,max}$, and is estimated as

$$\eta \approx \frac{\pi^4}{15}\frac{E_0^4}{\ln 5}\left(\frac{L_{\rm PL}}{L_{\rm BB}}\right)_{\rm obs} \quad (2)$$

for $\alpha_{\rm X} = 2$, and

$$\eta \approx \frac{\pi^4}{15} E_0^4 2^{\alpha_{\rm X}-1}(\alpha_{\rm X}-2)[1-5^{-(\alpha_{\rm X}-2)}]\left(\frac{L_{\rm PL}}{L_{\rm BB}}\right)_{\rm obs} \quad (3)$$

for $\alpha_{\rm X} \neq 2$. For the typical parameters of $E_0 \sim 0.5$ keV, $\alpha_{\rm X} \sim 2$, and $(L_{\rm PL}/L_{\rm BB})_{\rm obs} \sim 1$ of SGRs, we have $\eta \sim 4.0 E_0^4$. It should be pointed out that the minimum energy (E_1) of the nonthermal component of the distribution cannot be determined by using available X-ray data because of the effect of the interstellar absorption. However, E_1 cannot be smaller than E_0 according to the model of Thompson et al. (2002). We arbitrarily set $E_1 = 1$ keV.

Because the spectral distribution of the soft photons satisfies equation (1), we can estimate the typical energy of the X-rays by using $\langle E_{\rm X}\rangle = \int F_{\rm X}(E_{\rm X}) E_{\rm X}\, dE_{\rm X} / \int E_{\rm X}(E_{\rm X})\, dE_{\rm X}$, which gives

$$\langle E_{\rm X}\rangle = \frac{E_0^4\pi^4/15 + \eta\int_{E_1}^{E_{\rm X,max}} E_{\rm X}^{-\alpha_{\rm X}+1}\, dE_{\rm X}}{2E_0^3\zeta(3) + \eta\int_{E_1}^{E_{\rm X,max}} E_{\rm X}^{-\alpha_{\rm X}}\, dE_{\rm X}}, \quad (4)$$

where $\zeta(x)$ is the zeta function and $\zeta(3) \approx 1.2$. For $\alpha_{\rm X} = 2$ and $E_0 = 0.5$ keV, we have $\langle E_{\rm X}\rangle \approx 2.84$ keV for $E_{\rm X,max} = 100$ keV and $\langle E_{\rm X}\rangle \approx 2.32$ keV for $E_{\rm X,max} = 30$ keV. Generally, since the optical depth $\tau(\theta)$ is anisotropic for the resonant cyclotron scattering, meaning that the emission leaving the surface of the neutron star near equatorial plane will be strongly scattered at the cyclotron resonance while at the poles the emission will emerge almost unscattered (Thompson et al. 2002), $\langle E_{\rm X}\rangle$ should be a function of the polar angle (θ), although the detailed dependence of the emerging spectrum on θ is not given in the model of Thompson et al. (2002). In fact, in a dipole field, the resonance radius in the approximation of static charges is proportional to $[1-(3/4)\sin^2\theta]^{1/6}$, so the emerging spectrum and thus $\langle E_{\rm X}\rangle$ depend on the θ. On the other hand, for the

thermal emission, the temperature is also a function of polar angle θ. For example, the temperature distribution on the stellar surface for a cooling neutron star with a strong magnetic dipole is $T_s(\theta) \propto [\cos^2\theta/(3\cos^2\theta+1)^{0.8}]$ (Heyl & Hernquist 1998). Cheng & Zhang (2001) have shown that the fractional size of the outer gap has a weak dependence on the polar angle θ at a certain angular range (say, 0°–60°). Therefore, for simplicity, we ignore the dependence of the average X-ray energy $\langle E_X\rangle$ on the polar angle and estimate it using equation (4).

2.2. *The Outer Gap*

In magnetar models, the quiescent X-ray emission from SGRs and the persistent pulsed X-ray emission of the anomalous X-ray pulsars may be powered by internal heating produced by the decay of the strong magnetic fields (Usov 1992, 1997; Thompson & Duncan 1993). This thermal X-ray power is much higher than the spin-down power of the SGRs. Because of the strong magnetic field near the stellar surface, the high-energy γ-ray emission cannot be produced at the polar gap. However, the outer gap far from the stellar surface may exist, and high-energy γ-rays may be produced inside the outer gap. Here, we consider the mechanism for sustaining the outer gap.

According to Zhang & Cheng (1997), the parallel electric field in the outer gap can be approximated as

$$E_{\parallel} = f^2 B(r)\left(\frac{r}{R_L}\right)^{1/2}, \tag{5}$$

where f is the fractional size of the outer gap, $B(r)$ is the magnetic field strength at the radius, r, to the star, and R_L is the radius of the light cylinder. This electric field will accelerate the electrons/positrons to relativistic energy in the outer gap. Because these accelerated particles will lose their energy through synchrocurvature radiation (Cheng & Zhang 1996), their Lorentz factor is given by (Zhang & Cheng 1997)

$$\gamma(r) \approx 2.0\times10^7 f^{1/2} B_{12}^{1/4} P^{-1/4}\left(\frac{r}{R_L}\right)^{-3/8} R_6^{3/4}, \tag{6}$$

where $B_s = 10^{12}B_{12}$ G is the surface magnetic field, P is the pulsar period in seconds, and R is the stellar radius in 10^6 cm. The characteristic energy of the γ-ray photons in the outer gap can be approximated as

$$E_\gamma \approx 5.0\times10^7 f^{3/2} B_{12}^{3/4} P^{-7/4} R_6^{9/4}\left(\frac{r}{R_L}\right)^{-13/8} \text{ eV}. \tag{7}$$

Since there is X-ray emission with large X-ray luminosity from the stellar surface in the magnetar, these X-rays interact with high-energy photons to produce $e^{\pm}$ pairs through the photon-photon pair production process in the outer gap, sustaining the outer gap. This pair production condition is

$$\langle E_X\rangle E_\gamma\left[1-\cos(\theta_{X\gamma})\right] = 2(m_e c^2)^2, \tag{8}$$

where $\langle E_X\rangle$ is the typical energy of the X-rays, E_γ is given by equation (7), $m_e c^2$ is the electron rest energy, and $\theta_{X\gamma}$ is the directional angle between the high-energy photons and the X-rays. Generally, the fractional size of the outer gap can be estimated by using the above condition. Inserting equation (7) into equation (8), we have

$$f(r) \approx 1.4\left(\frac{B_s}{10^{14}\text{ G}}\right)^{-1/2}\left(\frac{P}{6\text{ s}}\right)^{7/6}\left(\frac{r}{R_L}\right)^{13/12}\left(\frac{\langle E_X\rangle}{\text{keV}}\right)^{-2/3} \times\left[\frac{2}{(1-\cos\theta_{X\gamma})}\right]^{2/3}\left(\frac{R}{15\text{ km}}\right)^{-3/2}. \tag{9}$$

In this equation, $\langle E_X\rangle$ is given by equation (4), and $\theta_{X\gamma}$ is estimated below.

In a two-dimensional static magnetic dipole with magnetic inclination angle α, the magnetic field in the polar coordinate is given by

$$\boldsymbol{B}(\boldsymbol{r}) = \frac{\mu}{r^3}[2\cos(\theta-\alpha)\hat{r} + \sin(\theta-\alpha)\hat{\theta}]l, \tag{10}$$

where μ is the magnetic moment, and $\hat{r}$ and $\hat{\theta}$ are the unit vectors of radial and polar angle directions, respectively. From this equation, the angle between the local radial direction and the magnetic field is determined by

$$\cos\psi = \frac{2\cos(\theta-\alpha)}{[3\cos^2(\theta-\alpha)+1]^{1/2}}. \tag{11}$$

The high-energy photons produced by the accelerated particles are emitted along the direction of the magnetic field lines in the outer gap. We assume uniform X-ray luminosity across all colatitudes, and therefore that the dominant contribution to the number of soft photons at any given location in the outer gap might come from those propagating radially. With such a assumption, the angle between the high-energy photons and the X-rays can be estimated. If the high-energy photons are emitted along the negative direction of the magnetic field (i.e., in the quasi–head-on geometry for the photon-photon collisions), we have

$$\theta_{X\gamma} = \pi - \psi. \tag{12}$$

It should noted that $\theta_{X\gamma} = \psi$ for the high-energy photons emitting along the positive direction of the magnetic field lines. In such a case, the threshold of the photon-photon pair production is much greater than that in the quasi–head-on case, so we neglect it here.

After estimating $\langle E_X\rangle$ and $\theta_{X\gamma}$, in principle, we can calculate the values of $f(r)$ at the radial distances from the inner boundary (which is the interception between the null charge surface and the first open field lines, with radius r_{in}) to the point tangent to the light cylinder (this radius is labeled r_c). An interesting case is the fractional size $f(r_{in})$ of the outer gap at the inner boundary of the outer gap. Generally, r_{in} is estimated by

$$\frac{r_{in}}{R_L} = \frac{\sin^2(\theta_{in}-\alpha)}{\sin\theta_c\sin^2(\theta_c-\alpha)}, \tag{13}$$

where θ_{in} is estimated by

$$\tan\theta_{in} = \tfrac{1}{2}\left(3\tan\alpha + \sqrt{9\tan^2\alpha+8}\right), \tag{14}$$

and θ_c is the polar angle at which the magnetic field is tangent to the light cylinder, which is

$$\tan\theta_c = -\frac{3}{4\tan\alpha}\left[1+\left(1+\frac{8\tan^2\alpha}{9}\right)^{1/2}\right]. \tag{15}$$

Obviously, $r_{\rm in}/R_L$ can be estimated if the magnetic inclination angle of a pulsar is given; $r_{\rm in}$ can also be approximated by $r_{\rm in}/R_L \sim 4/(9\tan^2\alpha)$ for $\alpha \geq 45^\circ$ (Halpern & Ruderman 1993) or $r_{\rm in}/R_L \sim 4(\pi/2-\alpha)^2/9$ (Romani 1996). Therefore, we have

$$f(r_{\rm in}) \approx 1.4\left(\frac{B_s}{10^{14}\ {\rm G}}\right)^{-1/2}\left(\frac{P}{6\ {\rm s}}\right)^{7/6}\left(\frac{r_{\rm in}}{R_L}\right)^{13/12} \times \left(\frac{\langle E_{\rm X}\rangle}{\rm keV}\right)^{-2/3}\left(\frac{R}{15\ {\rm km}}\right)^{-3/2} g_1(\alpha)\ , \quad (16)$$

where

$$g_1(\alpha) = \left[\frac{2\sqrt{3\cos^2(\theta_{\rm in}-\alpha)+1}}{\sqrt{3\cos^2(\theta_{\rm in}-\alpha)+1}+2\cos(\theta_{\rm in}-\alpha)}\right]^{2/3}\ . \quad (17)$$

It should be pointed out that the outer gap will not exist if $f(r_{\rm in}) > 1$.

In order to calculate the average spectrum of high-energy γ-rays from the outer gap, we need to estimate the average fractional size of the outer gap. Because the length of the outer gap along the magnetic field is from the inner boundary ($r_{\rm in}$) to the point tangent to the light cylinder (r_c), we integrate equation (9) over r from $r_{\rm in}$ to r_c and then divide it by $(r_c - r_{\rm in})$, which gives

$$\langle f\rangle \approx 1.4\left(\frac{B_s}{10^{14}\ {\rm G}}\right)^{-1/2}\left(\frac{P}{6\ {\rm s}}\right)^{7/6} \times \left(\frac{\langle E_{\rm X}\rangle}{\rm keV}\right)^{-2/3}\left(\frac{R}{15\ {\rm km}}\right)^{-3/2} g_2(\alpha)\ , \quad (18)$$

where

$$g_2(\alpha) = \frac{R_L}{r_c - r_{\rm in}} \times \int_{r_{\rm in}/R_L}^{r_c/R_L} u^{13/12}\left[\frac{2\sqrt{4-3a(\alpha)u}}{\sqrt{4-3a(\alpha)u}+\sqrt{1-a(\alpha)u}}\right]^{2/3} du\ , \quad (19)$$

with $a(\alpha) = \sin^2(\theta_c - \alpha)\sin\theta_c$ and

$$\frac{r_c}{R_L} = \frac{1}{\sin\theta_c}\ . \quad (20)$$

In Figure 1, we show the variations of $f(r_{\rm in})$ and $\langle f\rangle$ with the magnetic inclination angle for the set of parameters $P = 7$ s, $B = 5\times10^{14}$ G, $\alpha_{\rm X} = 2$, $E_0 = 0.5$ keV, and $R = 15$ km. We have considered two cases: $\langle E_{\rm X}\rangle = 2.84$ keV for $E_{\rm X,max} = 100$ keV and $\langle E_{\rm X}\rangle \approx 2.32$ keV for $E_{\rm X,max} = 30$ keV. It can be seen that (1) the fractional size of the outer gap at the inner boundary increases with the magnetic inclination angle, (2) the average fractional size depends weakly on the magnetic inclination angle, and (3) the fractional size of the outer gap increases with decreasing $E_{\rm X,max}$.

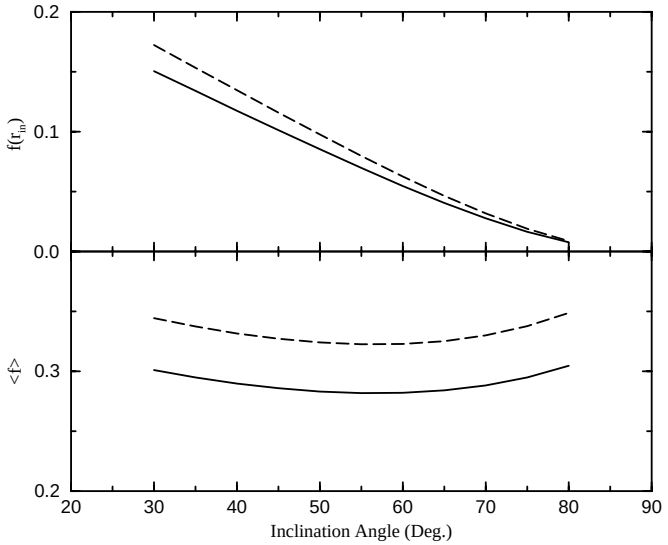

FIG. 1.—Fractional size of the outer gap varying with the magnetic inclination angle. *Top*: $f(r_{\rm in})$ vs. α. *Bottom*: $\langle f\rangle$ vs. α. The pulsar's parameters are $P = 7$ s and $B_{14} = 5$. Other parameters are $E_0 = 0.5$ keV, $\alpha_{\rm X} = 2$, and $(L_{\rm PL}/L_{\rm BB})_{\rm obs} = 1$. Solid and dashed curves show $E_{\rm X,max} = 100$ and 30 keV, respectively.

2.3. *Radiation Spectrum*

Cheng & Zhang (1996) studied the radiation from the charged particles in the curved magnetic field, and pointed out that the radiation would be described more accurately by a general radiation mechanism (they called it synchrocurvature radiation mechanism), in which the radiation is being emitted by the charged particles moving in a spiral trajectory along the curved magnetic field lines. As pointed out by Cheng & Zhang (1996), this mechanism differs from synchrotron and curvature mechanisms in general, but reduces to either synchrotron radiation when the pitch angle of the accelerated particles is not equal to zero and the curvature radius of the local magnetic field lines is infinite, or to curvature radiation when the pitch angle is zero, or to curvature radiation in some parametric regions (see Cheng & Zhang 1996 for details). In fact, when the synchrotron gyroradius $r_B = \gamma mc^2\sin\theta_p/eB(r)$ and the curvature radius of field $s \approx (rR_L)^{1/2}$ are of comparable probability, the synchrocurvature mechanism really provides a significant improvement, where γ is the Lorentz factor of the accelerated particles and θ_p is the pitch angle of the charged particles in the curved magnetic field. For magnetar field strengths, the condition for which this arises gives $r \sim 10^{11}(B_s/10^{14}\ {\rm G})^{2/5}\times(\gamma\sin\theta_p/10^6)^{-2/5}(R/10^6\ {\rm cm})^{6/5}$ cm. It clearly indicates a relatively small range of radii (depending on the γ assumed) for which the snychrocurvature mechanism is really more useful than the curvature radiation or synchrotron radiation. Zhang & Cheng (1997) used this mechanism to describe the production of nonthermal photons from the primary $e^\pm$ pairs along the curved magnetic field lines in the outer gap. The primary $e^\pm$ pairs have an approximate power-law distribution inside the outer gap because the energy and density of the primary $e^\pm$ pairs depend on local values of magnetic field, electric field, and radius of curvature. In steady state, the energy distribution of the accelerated particles in the outer gap is $(dN/dE_e) \propto E_e^{-16/3}$, where E_e is the energy of the accelerated particle. Here we use the synchrocurvature mechanism to describe the radiation from the

magnetar. Using the general formula of the synchrocurvature radiation power spectrum given by Cheng & Zhang (1996) and $(dN/dE_e)dE_e = (dN/dx)dx$, where $x = s/R_L$, the differential flux at the Earth is (Zhang & Cheng 1997)

$$F(E_\gamma) \approx \frac{1}{\Delta\Omega d^2}\frac{\dot{N}_0}{E_\gamma}\int_{x_{\min}}^{x_{\max}} x^{3/2}\frac{R_L}{R_c} \times \left[\left(1+\frac{1}{R_c^2Q_2^2}\right)F(y) - \left(1-\frac{1}{R_c^2Q_2^2}\right)yK_{2/3}(y)\right]dx , \quad (21)$$

where $\Delta\Omega$ is the solid angle of γ-ray beaming, d is the distance to the pulsar,

$$\dot{N}_0 = \sqrt{3}e^2\gamma_0 N_0/hR_L ,$$
$$N_0 \approx 1.4\times10^{30} f(B_{12}/P)R_6^3 ,$$
$$\gamma_0 \approx 2\times10^7\langle f\rangle^{1/2}(B_{12}/P)^{1/4} ,$$
$$R_c = xR_L/\{[1+r_B/(xR_L)]\cos^2\theta_p + (R_L/r_B)x\sin^2\theta_p\} ,$$
$$Q_2 = (1/xR_L)\{[(r_B/xR_L)+1-3(R_L/r_B)x] \times\cos^4\theta_p + 3(R_L/r_B)x\cos^2\theta_p + (R_L/r_B)^2x^2\sin^4\theta_p\}^{1/2} ,$$

and

$$\sin\theta_p \approx 0.79\langle f\rangle^{1/2}B_{12}^{-3/4}P^{7/4}x^{17/4} ,$$
$$F(y) = \int_y^\infty K_{5/3}(z)\,dz ,$$

where $K_{5/3}$ is the modified Bessel function of order 5/3, $y = E_\gamma/E_c$, and $E_c = (3/2)(\hbar c\gamma^3/x)(xQ_2)$ is the characteristic energy of the synchrocurvature photons. Here $x_{\min}$ and $x_{\max}$ are the minimum and maximum values of x; $x_{\min}$ can be estimated as $x_{\min} = (r_{\rm in}/R_L)^{1/2}$. Therefore, in this model there are two parameters, $\Delta\Omega$ and $x_{\max}$.

Furthermore, the position of resonant cyclotron scattering of ions or electrons is important for the pair production opacity. According to Thompson et al. (2002), ion cyclotron resonance occurs at 10–20 km, very close to the surface of the neutron star, and electron cyclotron resonance at ~50–100 km, about 5–10 radii of the neutron star. Obviously, it will significantly affect the pair production opacity. However, in the outer magnetosphere of the magnetar, which is far from the neutron star, the main pair production process is two-photon pair production. Because of the long period ($P = 5$–8 s) of the soft gamma-ray repeater, the inner boundary of the outer gap even for large magnetic inclination angle (say, 80°) is much greater than the location of the ions or electron cyclotron resonance. For example, using $r_{\rm in} = 4/9\tan^2\alpha$ (Halpern & Ruderman 1993), $P = 5$–8 s, and $\alpha = 80°$, we have $r_{\rm in} \sim (3.3$–$5.5)\times10^3$ km. Therefore, as a reasonable approximation, we ignore the effect of the position of resonant cyclotron scattering on the pair production process in our phase-averaged spectrum of high-energy γ-rays produced in the outer gap. In fact, the number density at any position (r) of the outer gap is approximated as $n_{\rm X} \sim L_{\rm X}/4\pi r^2\langle E_{\rm X}\rangle c$, where $L_{\rm X}$ is the X-ray luminosity and c is the light speed. The optical depth due to photon-photon pair production at a radial distance $\langle R\rangle$ is $\tau_{\gamma\gamma} \sim (\sigma_{\rm T}/3)n_{\rm X}\langle R\rangle$, which gives

$$\tau_{\gamma\gamma} \sim 8\times10^{-3}\left(\frac{L_{\rm X}}{10^{35}\ {\rm ergs\ s^{-1}}}\right) \times\left(\frac{P}{5\ {\rm s}}\right)^{-1}\left(\frac{\langle E_{\rm X}\rangle}{\rm keV}\right)^{-1}\left(\frac{\langle R\rangle}{R_L}\right)^{-1} , \quad (22)$$

where $\sigma_{\rm T}$ is the Thomson cross section and $\langle R\rangle$ is the order of R_L [$R_L \sim 2.5\times10^{10}$ cm for a typical period ($P = 5$ s) of an SGR]. Because the production region of high-energy γ-rays is far away from the stellar radius, the position of the resonant cyclotron scattering has little effect on photon-photon pair production from equation (22). Moreover, from equation (22), the optical depth is small, so that most high-energy γ-rays can escape from the outer gap.

Furthermore, the integral flux with energy greater than a certain value E_i is given by

$$F(\geq E_i) = \int_{E_i}^{E_{\max}} F(E_\gamma)\,dE_\gamma , \quad (23)$$

where $E_{\max}$ is the maximum energy of γ-rays. Finally, the γ-ray luminosity provided by the outer gap is

$$L_\gamma \approx 4.0\times10^{32}\left(\frac{\langle f\rangle}{0.5}\right)^3\left(\frac{B}{10^{14}\ {\rm G}}\right)^2 \times\left(\frac{P}{6\ {\rm s}}\right)^{-4}\left(\frac{R}{15\ {\rm km}}\right)^6 {\rm ergs\ s^{-1}} . \quad (24)$$

It should be pointed out that the form of equation (24) is the same as that given by Cheng & Zhang (2001), but there is a real difference between them. Compared to the γ-ray luminosity given by Cheng & Zhang (2001), $\langle f\rangle$ is given by equation (18). In this equation, $\langle E_{\rm X}\rangle$ is estimated by equation (13), in which the nonthermal component has been taken into account, and a function of the magnetic inclination angle, $g_2(\alpha)$, appears in equation (13).

As an example, we calculate the expected γ-ray fluxes using the typical parameters of the anomalous X-ray pulsars. In our calculations, $x_{\max} = 2$ is assumed. The expected γ-ray spectrum for a given pulsar is normalized so that the value of the integral $\Delta\Omega d^2\int_{E_{\min}}^{E_{\max}} E_\gamma F(E_\gamma)\,dE_\gamma$ equals the value given by equation (24), where $E_{\min}$ and $E_{\max}$ are the minimum and maximum energies of the γ-rays; here we set $E_{\min} = 1$ MeV and $E_{\max} = 100$ GeV. Figure 2 shows the expected γ-ray fluxes of a pulsar with $P = 7$ s, $B = 5\times10^{14}$ G, $E_0 = 0.5$ keV, $\alpha_{\rm X} = 2$, $E_{\rm X,max} = 100$ keV, and $R = 15$ km for four different magnetic inclination angles of 30°, 45°, 60°, and 75°. It can be seen that the spectrum extends to a higher energy range as the magnetic inclination angle increases. This result is a natural consequence of the outer gap geometry. As the magnetic inclination angle increases, there are two effects on the radiation spectrum. First, oblique rotators should give smaller mean angles between soft photons and hard γ-rays (a contention that depends on the latitudinal distribution of the soft photons), so that the pair production threshold move to higher energies. Second, since $x_{\min} = (r_{\rm in}/R_L)^{1/2}$ is a decreasing function of the magnetic inclination angle and $E_e \propto x^{-3/4}$ (Zhang & Cheng 1997), an increase in the magnetic inclination angle results in an increase of the accelerated particle's energy. In other words,

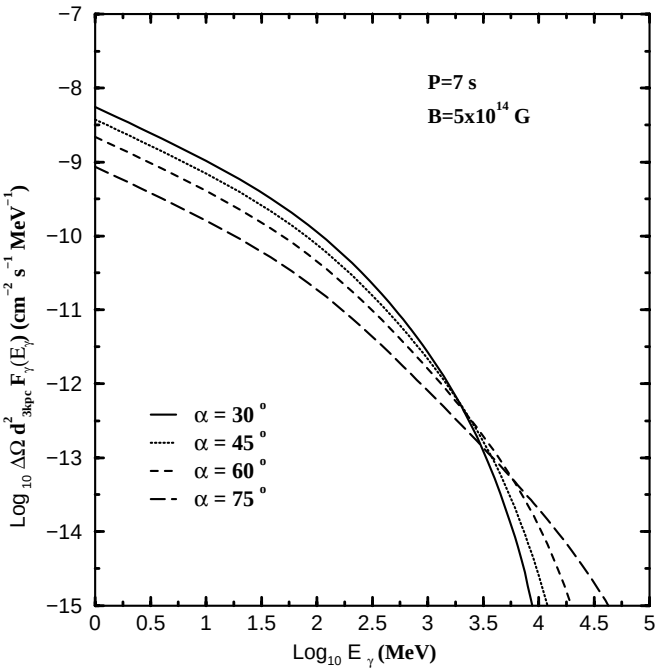

FIG. 2.—Expected γ-ray spectra of a pulsar with $P = 7$ s, $B_{14} = 5$ for different magnetic inclination angles. Other parameters are $E_0 = 0.5$ keV, $\alpha_X = 2$, $(L_{PL}/L_{BB})_{obs} = 1$ and $E_{X,max} = 100$ keV. The solid, dotted, dashed, and long dashed curves represent the expected γ-ray fluxes for the magnetic inclination angles of 30°, 45°, 60°, and 75°, respectively.

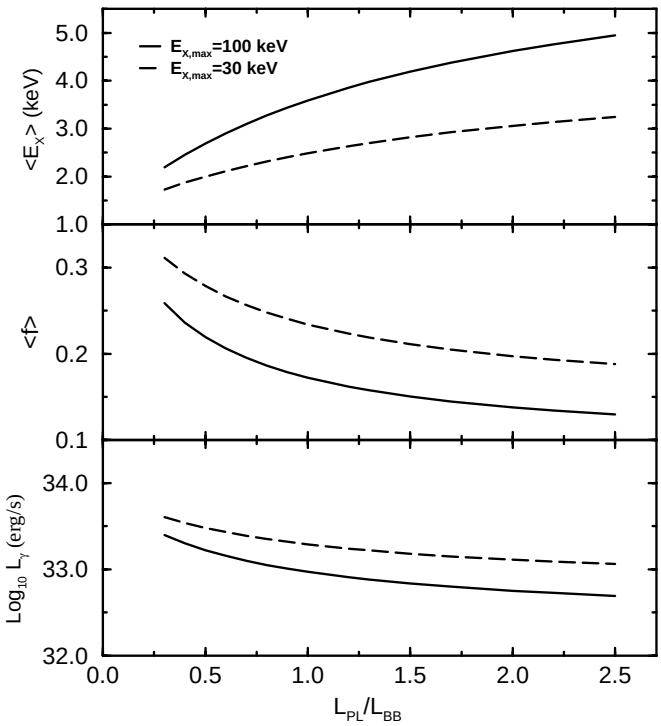

FIG. 3.—Variations of average X-ray energy ($\langle E_X \rangle$), average fractional size of outer gap ($\langle f \rangle$) and γ-ray luminosity (L_γ) of SGR 1806−20 with $(L_{PL}/L_{BB})_{obs}$ for $E_{X,max} = 100$ and 30 keV, respectively, where $\alpha = 80°$ and $R = 15$ km are assumed.

the energy interval ($\Delta E = E_{max} - E_{min}$, where $E_{max} \propto x_{min}^{-3/4}$ and $E_{min} \propto x_{max}^{-3/4}$) of the accelerated particles becomes large as the magnetic inclination angle increases; therefore, the γ-ray fluxes extend to higher energies as the dipole obliquity increases.

3. APPLICATIONS TO SGRs

Although four SGRs have been identified, the data are still lacking for SGR 1627−41. For SGR 1806−20 and SGR 1900+14, both the periods and period derivatives have been determined, and the spectral data in their quiescent states have been given. Therefore, we apply this model to SGR 1806−20 and SGR 1900+14.

3.1. *SGR 1806−20*

For SGR 1806−20, the period and period derivative are 7.47 s and 2.8×10^{-11} s s^{-1}, respectively; assuming a magnetic dipole radiation, the dipolar magnetic field strength is 8×10^{14} G (Kouveliotou et al. 1998). Because of the association of SGR 1806−20 with supernova remnant (SNR) G10.0−0.3, the distance to this SGR is ∼14 kpc (Kulkarni et al. 1994). Using *ASCA* data, Perna et al. (2001) pointed out that the temperature of the thermal component is not determined, because of too few soft X-ray counts. However, Marsden & White (2001) estimated the temperature ($E_0 = kT \sim 0.45$) and photon index ($\alpha_X \sim 1.7$) using a blackbody plus power-law model. They also estimated the ratio of the 2–10 keV power law and bolometric blackbody luminosities, $(L_{PL}/L_{BB})_{obs} \sim 1.3$. We use the data given by Marsden & White (2001) to estimate the average X-ray energy $\langle E_X \rangle$ in equation (4). From the data given by Marsden & White, we have $E_0 \approx 0.45$ keV and $\alpha_X \approx 1.7$. However, the $(L_{PL}/L_{BB})_{obs}$ changes from ∼0.3 to ∼2.5. In Figure 3, we show the variations of $\langle E_X \rangle$, $\langle f \rangle$, and γ-ray luminosity (L_γ) with $(L_{PL}/L_{BB})_{obs}$ for $E_{X,max} = 100$ and 30 keV respectively, where we assume that $\alpha = 80°$ and $R = 15$ km. Obviously, the increase of $(L_{PL}/L_{BB})_{obs}$ results in an increase of $\langle E_X \rangle$ and a decrease of $\langle f \rangle$ and L_γ. In our calculations, the average fractional sizes of the outer gap and the γ-ray luminosity are given by equations (18) and (24).

We now consider the integral flux of high-energy γ-rays produced in the outer gap of SGR 1806−20. Since the radiation spectrum for a larger magnetic inclination angle will extend to a higher energy region, we consider the case for $\alpha = 80°$. In this case, $r_{in} \sim 9.5 \times 10^8$ cm, which is far from the stellar surface, so the dipole approximation is valid. Because of the uncertainties of $(L_{PL}/L_{BB})_{obs}$ and $E_{X,max}$, we calculate the integral fluxes of high-energy γ-rays of SGR 1806−20 for $(L_{PL}/L_{BB})_{obs}$ =0.3, 1.3, and 2.5 and $E_{X,max} = 30$ and 100 keV. Here $\langle f \rangle \approx 0.36$, 0.27, and 0.24 when $E_{X,max} = 30$ keV and 0.31, 0.21, and 0.18 when $E_{X,max} = 100$ keV for $(L_{PL}/L_{BB})_{obs} = 0.3$, 1.3, and 2.5. The expected integral fluxes are shown in Figure 4, where the beaming solid angle of γ-rays is assumed to be 1 sr. For a given $E_{X,max}$, we show the change range of the integral fluxes due to the uncertainties of the $(L_{PL}/L_{BB})_{obs}$ from ∼0.3 to ∼2.5. For comparison, we also show the sensitivities of EGRET, GLAST, MAGIC, and VERITAS (Catanese & Weekes 1999). According to our model, GLAST, MAGIC, and VERITAS will not detect the γ-rays from this SGR if $E_{X,max}$ is greater than 30 keV.

3.2. *SGR 1900+14*

For SGR 1900+14 with $P = 5.18$ s and $\dot{P} = 6.1 \times 10^{-11}$ s s^{-1}, the dipolar magnetic field strength is 2×10^{14} G (Hurley

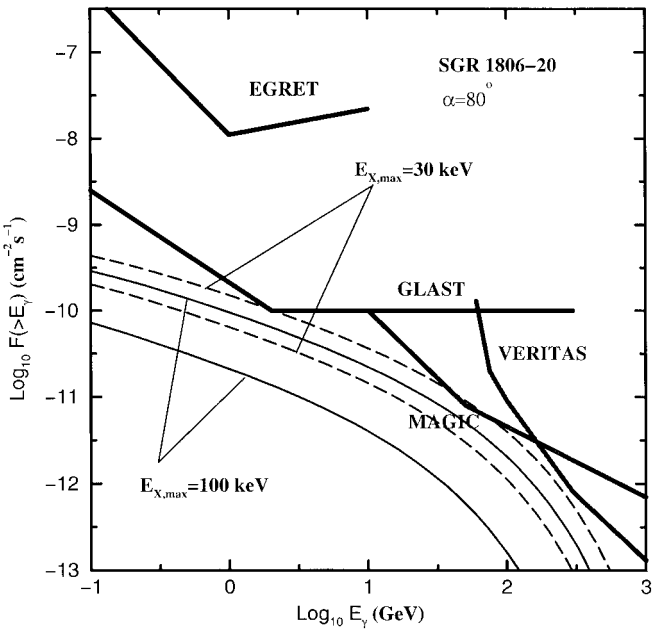

FIG. 4.—Variation ranges of the expected integral fluxes of SGR 1806−20. The uncertainties of the $(L_{PL}/L_{BB})_{obs}$ from ∼0.3 to ∼2.5. Two cases of $E_{X,max} = 100$ and 30 keV are considered, the beaming solid angle of γ-rays is assumed to be 1 sr. For comparison, the sensitivities of EGRET, GLAST, MAGIC, and VERITAS (Catanese & Weekes 1999) are also shown.

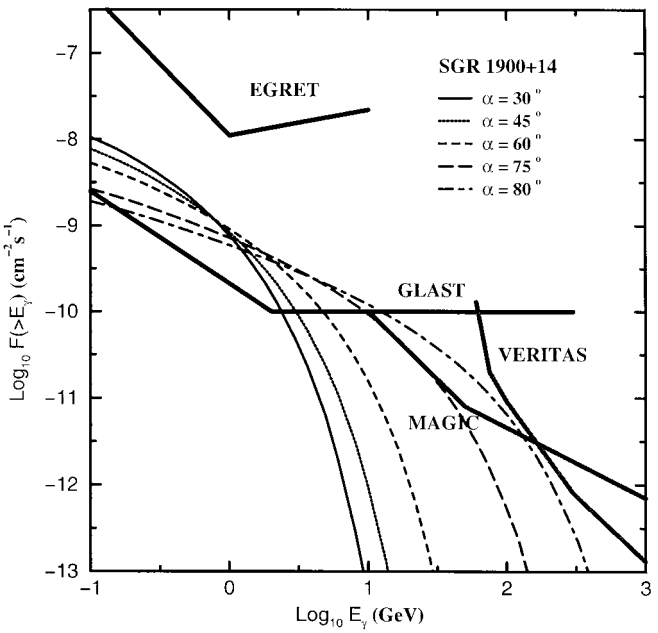

FIG. 5.—Expected integral fluxes of γ-rays from SGR 1900+14 for different inclination angles. The parameters are $(L_{PL}/L_{BB})_{obs} = 1$, $E_{X,max} = 100$ keV, and the beaming solid angle of γ-rays is assumed to be 1 sr. For comparison, the sensitivities of EGRET, GLAST MAGIC, and VERITAS are also shown.

et al. 1999). It has been shown that SGR 1900+14 is associated with SNR G42.8+0.6; then the distance to this SGR is about 5 kpc (Kouveliotou et al. 1994; Hurley et al. 1999). Using *BeppoSAX* observation of SGR 1900+14 in a quiescent period, Woods et al. (1999) estimated $E_0 = kT = 0.51$ keV and $\alpha_X = 2.1$ by using the blackbody plus power-law model. Perna et al. (2001) fitted *ASCA* observed data using the blackbody plus power-law model and estimated that $E_0 = 0.53$ keV and $\alpha_X = 2.1$. Marsden & White (2001) also fitted the *ASCA* data. They estimated that $E_0 \approx 0.4$ keV and $\alpha_X \approx 1.9$, and the value of $(L_{PL}/L_{BB})_{obs}$ changes from ∼0.62 to ∼1.5. It has been shown that the different values of $(L_{PL}/L_{BB})_{obs}$ result in different values of $\langle f \rangle$. In our calculations, we use the values of E_0 and α_X given by Marsden & White (2001).

Using the above parameters, the average X-ray energy and average fractional size of the outer gap are estimated for a given magnetic inclination angle. First we set $(L_{PL}/L_{BB})_{obs} = 1$ and $E_{X,max} = 100$ keV, and then we consider the dependence of the γ-ray integral fluxes of SGR 1900+14 on the magnetic inclination angle. We calculate the γ-ray integral fluxes for $\alpha = 30°$, 45°, 60°, 75°, and 80° and show the results in Figure 5, where the beaming solid angle of γ-rays is assumed to be 1 sr. For comparison, we also show the sensitivities of EGRET, GLAST, MAGIC, and VERITAS (Catanese & Weekes 1999). It can be seen that the expected γ-ray integral flux is greater than the sensitivity of GLAST, and especially greater than the sensitivities of both GLAST and MAGIC if the magnetic inclination angle is not less than 80°. Furthermore, we consider the effect of the uncertainties of $(L_{PL}/L_{BB})_{obs}$ and $E_{X,max}$ on the γ-ray integral flux of SGR 1900+14. Because the decrease of $(L_{PL}/L_{BB})_{obs}$ or/and $E_{X,max}$ makes $\langle f \rangle$ increase, it is necessary to check the maximum integral flux in a reasonable parameter range. For $E_{X,max} = 100$ and 30 keV, we calculate the γ-ray integral fluxes for $\alpha = 30°$ and 80°, respectively, when $(L_{PL}/L_{BB})_{obs} = 0.62$, which give the upper values of the expected γ-ray integral fluxes of SGR 1900+14. The results are shown in Figure 6. From this figure, the expected γ-ray integral flux for $E_{X,max} = 30$ keV, $\alpha = 80°$, and $(L_{PL}/L_{BB})_{obs} \approx 0.62$ is greater than the sensitivities of

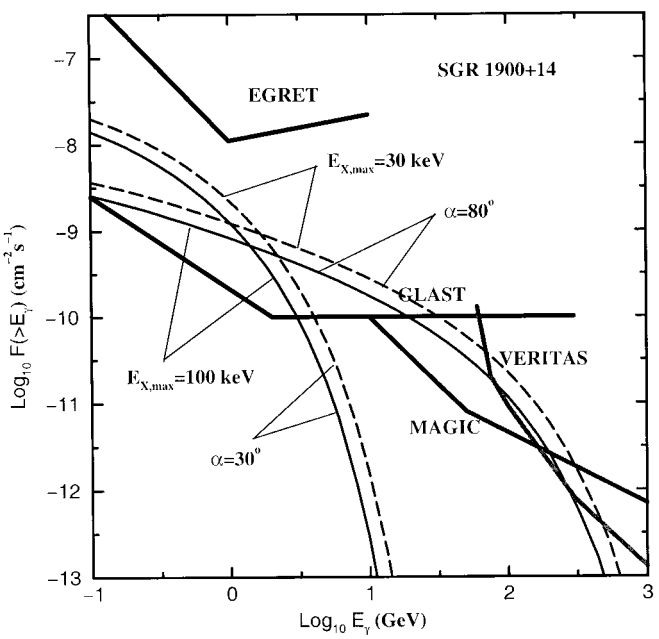

FIG. 6.—Expected integral fluxes of γ-rays from SGR 1900+14 for $\alpha = 30°$ and 80° and $E_{X,max} = 100$ and 30 keV. The parameters are $(L_{PL}/L_{BB})_{obs} = 0.62$, and the beaming solid angle of γ-rays is assumed to be 1 sr. For comparison, the sensitivities of EGRET, GLAST, MAGIC, and VERITAS are also shown.

GLAST, MAGIC, and VERITAS. However, our expected results are below the sensitivity of EGRET.

4. DISCUSSION

We have described a model for the high-energy γ-ray emission from the outer gap of a neutron star with a strong magnetic field. In this model, X-rays come from the stellar surface. The emerging X-ray spectrum will have a power-law tail because of multiple scattering at the cyclotron resonance in the magnetosphere (Thompson et al. 2002). Since there is not a detailed calculation for the emerging X-ray spectrum, we have constructed the X-ray field based on the observed data of SGRs and the ideas of Thompson et al. (2002). This X-ray field provides a soft photon source in which the outer gap is sustained. The outer gap is sustained by the collision between these X-rays and the high-energy photons produced in the outer gap through photon-photon pair production. Taking a two-dimensional dipole geometry into account, we estimated the fractional size of the outer gap. The fractional size of the outer gap depends on the period, surface magnetic field, average X-ray energy, and the magnetic inclination angle of the pulsar. We have given the fractional size of the outer gap at the inner boundary, $f(r_{\rm in})$, and pointed out that the outer gap exists when $f(r_{\rm in}) \leq 1$ (see eq. [16]). We also estimated the average fractional size of the outer gap (see eq. [18]) to explain the average spectrum and luminosity of high-energy γ-rays. For a given SGR, the fractional size of the outer gap at the inner boundary of the outer gap decreases with the magnetic inclination angle; however, the average fractional size of the outer gap indicates a concave shape with the magnetic inclination angle (see Fig. 1). We have calculated the γ-ray spectra for given typical parameters of the SGR; the spectrum extends to a higher energy range as the magnetic inclination angle increases (see Fig. 2).

In this model, we have considered two possible values of X-ray maximum energy ($E_{\rm X,max}$) according to Thompson et al. (2002), i.e., $E_{\rm X,max} \sim 100$ keV for the electron cyclotron scattering and $\sim$30 keV for the ion cyclotron scattering. As pointed out by Thompson et al. (2002), however, which cyclotron scattering works depends on further observations, especially in the energy range 20–500 keV. The uncertainty of $E_{\rm X,max}$ affects the average X-ray energy, $\langle E_{\rm X}\rangle$. For example, in the case of $E_0 = 0.5$ keV, $\alpha_{\rm X} = 2$, and $(L_{\rm PL}/L_{\rm BB})_{\rm obs} = 1$, $\langle E_{\rm X}\rangle \approx 2.84$ keV for $E_{\rm X,max} = 100$ keV and $\langle E_{\rm X}\rangle \approx 2.32$ keV for $E_{\rm X,max} = 30$ keV; the ratio is $2.84/2.32 \sim 1.22$. From equation (18), $\langle f\rangle \propto \langle E_{\rm X}\rangle^{-2/3}$, so the corresponding ratio is $(2.84/2.32)^{-2/3} \sim 0.87$. This will further affect the γ-ray luminosity, since $L_\gamma \propto \langle f\rangle^3 \propto \langle E_{\rm X}\rangle^{-2}$ (the corresponding ratio is $\sim$0.67).

This model has been applied to describe high-energy emissions from SGR 1806−20 and SGR 1900+14. For SGR 1806−20, we have considered the effect of $(L_{\rm PL}/L_{\rm BB})_{\rm obs}$ on $\langle E_{\rm X}\rangle$, $\langle f\rangle$, and L_γ because the change range of $(L_{\rm PL}/L_{\rm BB})_{\rm obs}$ is from $\sim$0.3 to $\sim$2.5 (Marsden & White 2001). The $\langle E_{\rm X}\rangle$ increases with $(L_{\rm PL}/L_{\rm BB})_{\rm obs}$, while $\langle f\rangle$ and L_γ decrease with $(L_{\rm PL}/L_{\rm BB})_{\rm obs}$ (see Fig. 3). The expected integral γ-ray fluxes for SGR 1806−20 are below the threshold of GLAST. It should be noted that in our calculations we have used the observed data given by Marsden & White (2001). However, Perna et al. (2001) pointed out that there were too few soft counts to allow meaningful constraints on the fit parameters for the thermal component of SGR 1806−20. For SGR 1900+14, our model results indicate that SGR 1900+14 may be detected by GLAST, and may be detected by GLAST, MAGIC, or even VERITAS if SGR 1900+14 has a larger magnetic inclination angle (say, 80°; see Figs. 5 and 6). Again, in our calculation we have used the observed data given by Marsden & White (2001). In fact, Woods et al. (1999) estimated $E_0 = kT = 0.51$ and $\alpha_{\rm X} = 2.1$, which differ from those given by Marsden & White (2001). From Woods et al. (1999), we can obtain $(L_{\rm PL}/L_{\rm BB})_{\rm obs} \sim 1.3$. Using equation (4), we have $\langle E_{\rm X}\rangle \approx 2.83$ keV for $E_{\rm X,max} = 100$ and 2.18 keV for $E_{\rm X,max} = 30$ keV; these values are consistent with those (2.82 and 2.18 keV) based on the observed data given by Marsden & White (2001). Briefly, SGR 1900+14 is visible to GLAST, whereas SGR 1806−20 is not in our model, the main reason being that the latter is about 3 times more distant from the Earth.

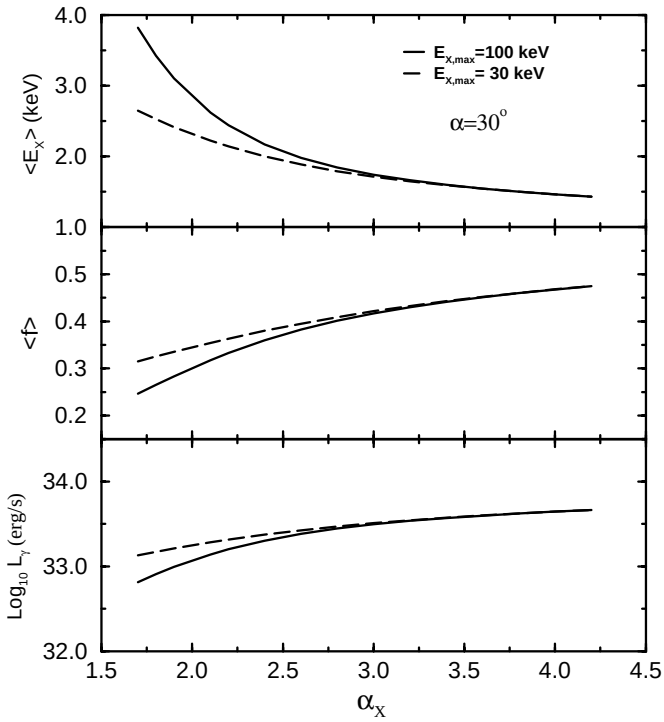

FIG. 7.—Dependence of average X-ray energy, average fractional size of the outer gap, and γ-ray luminosity on the photon index. The parameters are $P = 7$ s, $B = 5 \times 10^{14}$ G, $E_0 = 0.5$ keV, $(L_{\rm PL}/L_{\rm BB})_{\rm obs} = 1$, and $\alpha = 30°$.

In the magnetar model, SGRs are related to AXPs (Duncan & Thompson 1992; Thompson & Duncan 1996; Thompson et al. 2002). The fits to the spectra of AXPs indicate that the spectra of some AXPs have very soft power-law components (photon index $\sim$−4; see, e.g., Perna et al. 2001; Marsden & White 2001). Although the spectra of AXPs can be explained by passive radiative transport through the surface of a neutron star with a strong magnetic field (e.g., Özel 2001; Özel, Psaltis, & Kaspi 2001), multiple resonant scattering in the magnetar magnetosphere can also explain the AXP spectra (Thompson et al. 2002). Marsden & White (2001) have fitted the spectra of five AXPs using the blackbody plus power-law model (see also Perna et al. 2001). In principle, we can use the observed data given by Marsden & White (2001) to estimate average fractional sizes of the outer gap and γ-ray luminosities for these AXPs. Here we want to show the effect of different photon indices

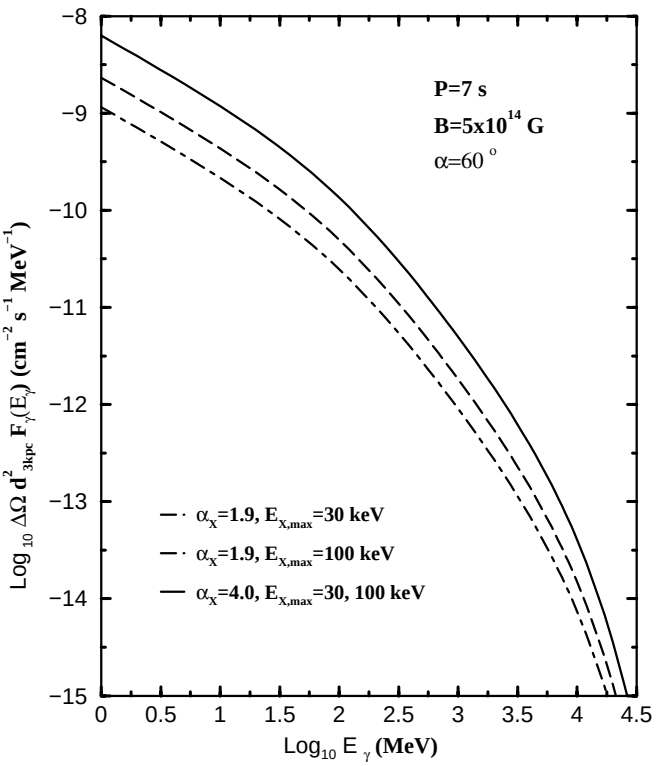

FIG. 8.—Expected γ-ray spectra of a pulsar with $P = 7$ s, $B_{14} = 5$ for different X-ray spectral indices and different maximum X-ray energies. The parameters are $E_0 = 0.5$ keV, $(L_{\rm PL}/L_{\rm BB})_{\rm obs} = 1$, and $\alpha = 60^\circ$.

on the average fractional sizes of the outer gap. In order to do so, we assume that $P = 7$ s, $B = 5 \times 10^{14}$ G, $E_0 = 0.5$ keV, and $(L_{\rm PL}/L_{\rm BB})_{\rm obs} = 1$. The expected results are shown in Figure 7, where two cases of $E_{\rm X,max} = 100$ and 30 keV are considered. It can be seen that (1) $\langle E_{\rm X}\rangle$ decreases with increasing $\alpha_{\rm X}$ and approaches $3kT \sim 1.5$ keV when $\alpha_{\rm X}$ tends to $\sim$4, and (2) $\langle f\rangle$ and L_γ increase with $\alpha_{\rm X}$ and approach the same values for different values of $E_{\rm X,max}$ when $\alpha_{\rm X}$ tends to $\sim$4. If the basic parameters of an AXP are the same as those of an SGR, it means that the AXP has greater $\langle f\rangle$ and L_γ, and is more easily detected. In Figure 8, we show the high-energy γ-ray spectra of a magnetar with different X-ray spectral indices for $E_{\rm X,max} = 30$ and 100 keV, respectively. In our calculations, the basic parameters are $P = 7$ s, $B = 5 \times 10^{14}$ G, $E_0 = 0.5$ keV, $(L_{\rm PL}/L_{\rm BB})_{\rm obs} = 1$, and $\alpha = 60^\circ$. The high-energy γ-ray spectrum from the magnetar with a small $\alpha_{\rm X}$ (say, 1.9) depends on the $E_{\rm X,max}$, and is less than that from the magnetar with a large $\alpha_{\rm X}$ (say, 4). Furthermore, the high-energy γ-ray spectrum of the magnetar with a large $\alpha_{\rm X}$ does not depends on the $E_{\rm X,max}$ (see Fig. 8). Again, we can see that the spectral index and the spectral break $E_{\rm X,max}$ play important roles in determining the γ-ray spectrum.

It is very important to note that the model average γ-ray spectra presented in this paper are the most plausible spectra of SGRs without knowing the magnetic inclination angle and the viewing angle. The "realistic"/"observed" spectra of SGRs obviously depend on those two angles. However, unless we are comparing the phase-dependent spectra with model spectra, the model average spectra should be close to the "observed" phase-averaged spectra of SGRs.

This work is partially supported by a RGC grant of the Hong Kong government, the National Nature Scientific Foundation of China (10073008), and the National 973 Projection of China (NKBRSFG 19990754).

REFERENCES

Baring, M. G., & Harding, A. K. 2001, ApJ, 547, 929
Catanese, M., & Weekes, T. C. 1999, PASP, 111, 1193
Cheng, K. S., & Zhang, J. L. 1996, ApJ, 463, 271
———. 2001, ApJ, 562, 918
Duncan, R. C., & Thompson, C. 1992, ApJ, 392, L9
Halpern, J. P., & Ruderman, M. 1993, ApJ, 415, 286
Heyl, J. S., & Hernquist, L. E. 1998, MNRAS, 297, L69
Heyl, J. S., & Kulkarni, S. R. 1998, ApJ, 506, L61
Hurley, K., et al. 1999, ApJ, 510, L111
———. 2000, in Proc. 5th Huntsville Symp. on Gamma-Ray Bursts, ed. R. M. Kippen, R. S. Mallozzi, & G. J. Fishman (New York: AIP), 763
Kouveliotou, C., et al. 1994, Nature, 328, 125
———. 1998, Nature, 393, 235
———. 1999, ApJ, 510, L115
Kulkarni, S. R., et al. 1994, Nature, 368, 129
Marsden, D., & White, N. E. 2001, ApJ, 551, L155
Mereghetti, S., & Stella, L. 1995, ApJ, 442, L17
Özel, F. 2001, ApJ, 563, 276
Özel, F., Psaltis, D., & Kaspi, V.M. 2001, ApJ, 563, 255
Perna, R., et al. 2001, ApJ, 557, 18
Romani, R. W. 1996, ApJ, 470, 469
Thompson, C., & Duncan, R. C. 1993, ApJ, 408, 194
———. 1996, ApJ, 473, 322
Thompson, C., Lyutikov, M., & Kulkarni, S. R. 2002, ApJ, 574, 332
Usov, V. 1992, Nature, 357, 472
———. 1997, A&A , 317, L87
Woods, P. M., et al. 1999, ApJ, 519, L139
Zhang, B. 2001, ApJ, 562, L59
Zhang, L., & Cheng, K. S. 1997, ApJ, 487, 370